Universal Occurrence of Soot Superaggregates with a Fractal Dimension of 2.6 in Heavily Sooting Laminar Diffusion Flames

W. Kim, C. M. Sorensen,* and A. Chakrabarti

Department of Physics, Kansas State University, Manhattan, Kansas 66506-2601

Received November 5, 2003. In Final Form: February 27, 2004

Using small-angle light scattering we show that a new phase of soot with size ca. 10 μm and a fractal dimension of $D \simeq 2.6$ exists in laminar diffusion flames for a wide range of heavily sooting fuels. This new phase appears to be a supramicrometer extension of the well-known submicrometer, $D \simeq 1.8$ phase of soot formed via diffusion-limited cluster aggregation (DLCA). The occurrence of this new soot phase correlates with an empirical sooting index for fuels. This supports a creation scenario in which these supramicrometer aggregates are created via a percolation of the submicrometer, $D \simeq 1.8$ aggregates.

I. Introduction

The formation of soot in hydrocarbon flames has many universal features that are independent of the fuel. The current picture of soot formation in theses flames[1,2] is that the heat of the flame pyrolyzes the fuel, breaking it down to smaller species including radicals, acetylene, and olefins. These species combine to form benzene rings, which in turn combine through mechanisms still being debated to form multiring polyaromatic hydrocarbons (PAH) of maximum thermodynamic stability. These ultimately condense into ca. 2−3 nm "tarry" droplets.[3−5] While these droplets grow through aggregation and coalesence and more surface reactions, the substance loses hydrogen to become the well-known soot primary particles:[6] roughly spherical particles with diameters typically in the 30−60 nm range composed of graphitic planes with a C/H ratio of ca. 8. Once formed, these primary particles continue to aggregate, but now without coalescence, through a process of diffusion-limited cluster aggregation (DLCA) in three dimensions (3D)[7] to form ramified fractal aggregates with a fractal dimension of $D \simeq 1.8$ into the submicron to micron scale.[8−12] It is these $D \simeq 1.8$ fractal aggregates that current wisdom believes to be the end product of fuel rich, hydrocarbon combustion.

In recent work we have studied soot formation in acetylene/air diffusion flames.[13,14] When burned in this manner, acetylene produces an unusually large amount of soot. Low in the flame, light scattering measurements showed typical submicron, $D \simeq 1.8$ soot aggregates. Higher in the flame, hence later in the soot growth process, light scattering showed supermicron, $D \simeq 2.6$ "superaggregates." These results are the first to suggest that a new phase of soot exists and led us to wonder how common this phase is. Below we show that this phase is common; it occurs in diffusion flames of fuels with high sooting tendency.

II. Experimental Method

In our experiments, static light scattering was used to measure the structure of the soot aggregates in the flames.[15] These measurements gave the scattered intensity $I(q)$ as a function of q, the scattering wave vector, $q = 4\pi\lambda^{-1} \sin(\theta/2)$, where λ is the optical wavelength and θ is the scattering angle. For aggregates with a fractal dimension greater than 2.0, $I(q)$ yields quantitative information regarding the size of the aggregate and fractal dimension of the aggregate's surface, which for both DLCA aggregates,[15] with $D \simeq 1.8$, and percolated aggregates,[16] with $D \simeq 2.55$, equals the bulk cluster fractal dimension.

An argon ion laser operating at $\lambda = 488$ nm was used as the light source. The detection apparatus was a small-angle light scattering device designed after Ferri[17] that allowed q values in the range $150\ \text{cm}^{-1} \le q \le 2.5 \times 10^4\ \text{cm}^{-1}$. This apparatus collects

* Corresponding author. E-mail: sor@phys.ksu.edu.

(1) Glassman, I. Soot Formation in Combustion Processes. 22nd Symposium (International) on Combustion, pp 295−311, The Combustion Institute, 1988.

(2) Frenklach, M. Reaction Mechanism of Soot Formation in Flames. *Phys. Chem. Chem. Phys.* **2002**, *4*, 2028−2037.

(3) D'Anna, A.; D'Alesso, A.; Minutolo, P. Spectroscopic and Chemical Characterization of Soot Inception. In *Soot Formation in Combustion: Mechanisms and Models*; Bockhorn, H., Ed.; Springer-Verlag: Heidelberg, 1994; pp 83−103.

(4) Dobbins, R. A.; Subramaniasiaviam, H. Soot Precursor Particles in Flames. In *Soot Formation in Combustion: Mechanisms and Models*; Bockhorn, H., Ed.; Springer-Verlag: Heidelberg, 1994; pp 290−301.

(5) Dobbins, R. A.; Fletcher, R. A.; Chang, H.-C. The Evolution of Soot Precursor Particles in a Diffusion Flame. *Combust. Flame* **1998**, *115*, 285−298.

(6) Lahaye, J.; Prado, G. In *Particulate Carbon: Formation During Combustion*; Siegla, D. C., Smith, G. W., Eds.; Plenum Press: New York, 1981; pp 33−55.

(7) Oh, C.; Sorensen, C. M. J. Light Scattering Study of Fractal Cluster Aggregation Near the Free Molecular Regime. *Aerosol Sci.* **1997**, *28*, 937−957.

(8) Samson, R. J.; Mulholland, G. W.; Gentry, J. W. Structural Analysis of Soot Agglomerates. *Langmuir* **1987**, *3*, 273−281.

(9) Zhang, H. X.; Sorensen, C. M.; Ramer, E. R.; Olivier, B. J.; Merklin, J. F. In Situ Optical Structure Factor Measurements of an Aggregating Soot Aerosol. *Langmuir* **1988**, *4*, 867−871.

(10) Megaridis, C. M.; Dobbins, R. A. Morphological Description of Flame Generated Materials. *Combust. Sci. Technol.* **1990**, *71*, 95−109.

(11) Sorensen, C. M.; Cai, J.; Lu, N. Light-Scattering Measurements of Monomer Size, Monomers Per Aggregate, and Fractal Dimension for Soot Aggregates in Flames. *Appl. Optics* **1992**, *31*, 6547−6557.

(12) Koylu, U. O.; Faeth, G. M. Structure of Overfire Soot in Buoyant Turbulent Diffusion Flames at Long Residence Times. *Combust. Flame* **1992**, *89*, 140−156.

(13) Sorensen, C. M.; Hagemann, W. B.; Rush, T. J.; Huang, H.; Oh, C. Aerogelation in a Flame Soot Aerosol. *Phys. Rev. Lett.* **1998**, *80*, 1782−1785.

(14) Sorensen, C. M.; Kim, W. G.; Fry, D.; Shi, D.; Chakrabarti, A. Observation of Soot Superaggregates with a Fractal Dimension of 2.6 in Laminar Acetylene/Air Diffusion Flames. *Langmuir* **2003**, *19*, 7560−7563.

(15) Sorensen, C. M. Light Scattering from Fractal Aggregates: A Review. *Aerosol Sci. Technol.* **2001**, *35*, 648−687.

(16) Strenski, P. N.; Bradley, P. M.; Debieve, J.-M. Scaling Behavior of Percolation Surfaces in Three-Dimensions. *Phys. Rev. Lett.* **1991**, *66*, 1330−1333.

(17) Ferri, F. Use of a Charge Coupled Device Camera for Low-Angle Elastic Light Scattering. *Rev. Sci. Instrum.* **1997**, *68*, 2265−2273.

10.1021/la036085+ CCC: $27.50
Published on Web 04/15/2004

Table 1. Fuels Used in This Study Along with Their Threshold Soot Index (TSI) from Olson et al.[31] [a]

fuel	TSI	superaggregates
	gases	
methane	~0	no
ethylene	0.7	no
acetylene	11	yes
	liquids	
hexadecane	~5.8	no
isooctane	6.4	no
1-hexadecene	11	no
JP5 jet fuel	-	marginal
decaline	15	marginal
toluene	44	yes
styrene	67	yes
1-methylnaphthalene	91	yes
	solids	
naphthalene	100	yes
polystyrene	-	likely
rubber	-	likely

[a] TSI values have an uncertainty of about ±20%. Also given is the observation of whether percolated superaggregates were observed. "Likely" means that superaggregates were not observed by light scattering, because the flame was not stable enough, but rather were inferred by a strong similarity in the soot produced in these flames to those that did show percolated superaggregates.

the scattered light with a high-quality lens, diameter 4.0 cm and focal length 6.0 cm, placed one focal distance from the flame in the forward direction of the incident laser beam. This beam passes through the lens and is eliminated with a small mirror at the focal point. A focal length 5.0 cm, *f*/2 camera lens behind the first lens images the Fourier plane of the first lens, which is one focal distance behind the first lens, onto a linear photodiode array. This array has 512 channels and is interfaced to a computer.

Direct observation of the very large soot in the flame and the flame structure was accomplished using a 10 power photomicroscope with an object distance of 15 cm. To obtain photographs, the flame was blacklit by a 7ns pulsed Nd:YAG laser with $\lambda =$ 532 nm shining on a white background behind the flame. This laser was triggered by the flash accessory of a digital camera that was part of the photomicroscope.

The flames were all laminar diffusion flames in ambient air. Gaseous fuels at controllable flow rates emanated from a brass tube with 0.9 cm inside diameter. Liquid fuels were burned with a simple wick burner with wick diameter of 0.6 cm. The burning rate was controlled by varying the length of the wick above a metal retaining cylinder. Solid fuels were burned as rods, or in the case of naphthalene, a candle 0.6 cm in diameter was fabricated. The fuels used are listed in Table 1.

III. Results

Scattering results for six of these flames are given in Figure 1. To interpret these graphs, realize that changes in slope on these double logarithmic graphs at a given q imply a length scale of the scattering system of ca. q^{-1}. A slope of 0 implies that all length scales of the system are smaller than q^{-1} in that range. A finite slope in a given q range implies a fractal morphology of the system over the corresponding size range q^{-1} with fractal dimension equal to the negative slope. For more detail on light scattering analysis, see ref 15.

In Figure 1 data for ethylene and isooctane (2,2,4-trimethylpentane) show weak scattering and, most significantly, a relatively flat, featureless $I(q)$ in the experimental q range. This implies that the soot aggregates that exist in these flames are smaller than the inverse of the largest q value measured, viz. $q(\max) = 2.5 \times 10^4$ cm^{-1}, implying $R_g \simeq 0.4\ \mu$m, where R_g is the soot cluster radius of gyration. The other four flames in Figure 1 also show the same flat $I(q)$ for low heights above the burner, h, which corresponds to early in the soot lifetime. This may again be interpreted to imply soot with $R_g \simeq 0.4\ \mu$m, and this has been confirmed for acetylene with large q measurements using a different detector where $D \simeq 1.8$ aggregates were seen.[14] However, with increasing h, the acetylene, toluene, 1-methylnaphthalene, and naphthalene flames in Figure 1 all display the same new feature in $I(q)$, namely, a 3 orders of magnitude increase in scattering in the q range from 150 to 10^4 cm^{-1}. For $q >$ 10^3 cm^{-1}, the feature slopes off linearly on these double logarithmic plots with a slope in the range from -2.5 to -2.7 and definitely less than 3.0. This scattering result implies the existence of ca. 10 μm aggregates (the inverse of q=10^3 cm^{-1}) with a fractal dimension of 2.6.

In our recent work on acetylene/air laminar diffusion flames,[14] we presented two scenarios for the formation of $D \simeq 2.6$ fractal aggregates in the flame: a percolation scenario and a restructuring scenario. In restructuring, one can propose that as the $D \simeq 1.8$ DLCA aggregates grow, they become more tenuous and hence more susceptible to restructuring in the shear flow of the flame. The colloid literature contains three examples of shear-induced restructuring with restructured fractal dimensions of $D \simeq 2.3-2.7$,[18−20] similar to the value we observe. In what follows, we argue in favor of the percolation scenario because of a correlation of the $D \simeq 2.6$ feature with fuel sooting tendency. Our results, however, do not conclusively eliminate the restructuring scenario, which must be investigated with future experiments.

Our recent work[14] included simulations that started with single, unaggregated spherical monomers. These monomers moved via a random walk (to simulate Brownian motion), and when they hit, they stuck together to create aggregates. This is the canonical DLCA simulation,[21,23] and we found $D \simeq 1.8$ aggregates formed. Our simulations were large enough (nearly one million monomers at volume fractions as low as 5×10^{-4} [23]) to allow the aggregation to proceed to the point where the aggregates filled the entire volume, a situation that must eventually happen whenever the cluster fractal dimension is less than the spatial dimension. At this point we found that the $D \simeq 1.8$ DLCA aggregates percolated to form larger "superaggregates" with fractal dimension of $D \simeq$ 2.6. This fractal dimension applies over length scales greater than the mean size of the $D \simeq 1.8$ aggregates that come together to form the superaggregate. These structures have also been seen in simulations by Gimel et al.[24,25] and Hasmy and Jullien.[26] It is well-known that a system of space-filling particles (or aggregates) will percolate at a filling threshold, and the resulting percolated cluster is

(18) Martin, J. E.; Wilcoxon, J. P.; Schaefer, D.; Odinek, J. Fast Aggregation of Colloidal Silica. *Phys. Rev. A* **1990**, *41*, 4379−4391.

(19) Carpineti, M.; Ferri, F.; Giglio, M.; Paganini, E.; Perini, U. Salt-Induced Fast Aggregation of Polystyrene Latex. *Phys. Rev. A* **1990**, *42*, 7347−7354.

(20) Jung, S. J.; Amal, R.; Raper, J. A. Monitoring Effects of Shearing on Floe Structure Using Small-Angle Light Scattering. *Power Technol.* **1996**, *88*, 51−54.

(21) Meakin, P. Formation of Fractal Clusters and Networks by Irreversible Diffusion-Limited Aggregation. *Phys. Rev.* **1983**, *51*, 1119−1122.

(22) Kolb, M.; Botet, R.; Jullien, R. Scaling of Kinetically Growing Clusters. *Phys. Rev. Lett.* **1983**, *51*, 1123−1126.

(23) Fry, D. Ph.D. Thesis, Kansas State University, 2003.

(24) Gimel, J. C.; Durand, D.; Nicolai, T. Transition between Flocculation and Percolation of a Diffusion-Limited Cluster-Cluster Aggregation Process using Three-Dimensional Monte Carlo Simulation. *Phys. Rev. B* **1995**, *51*, 11348−11357.

(25) Gimel, J. C.; Nicolai, T.; Durand, D. 3D Monte Carlo Simulations of Diffusion-Limited Cluster Aggregation up to the Sol−Gel Transition: Structure and Kinetics. *J. Sol-Gel Sci. Technol.* **1999**, *15*, 129−136.

(26) Hasmy, A.; Jullien, R. Percolation in Cluster-Cluster Aggregation Process. *Phys. Rev. E* **1996**, *53*, 1789−1794.

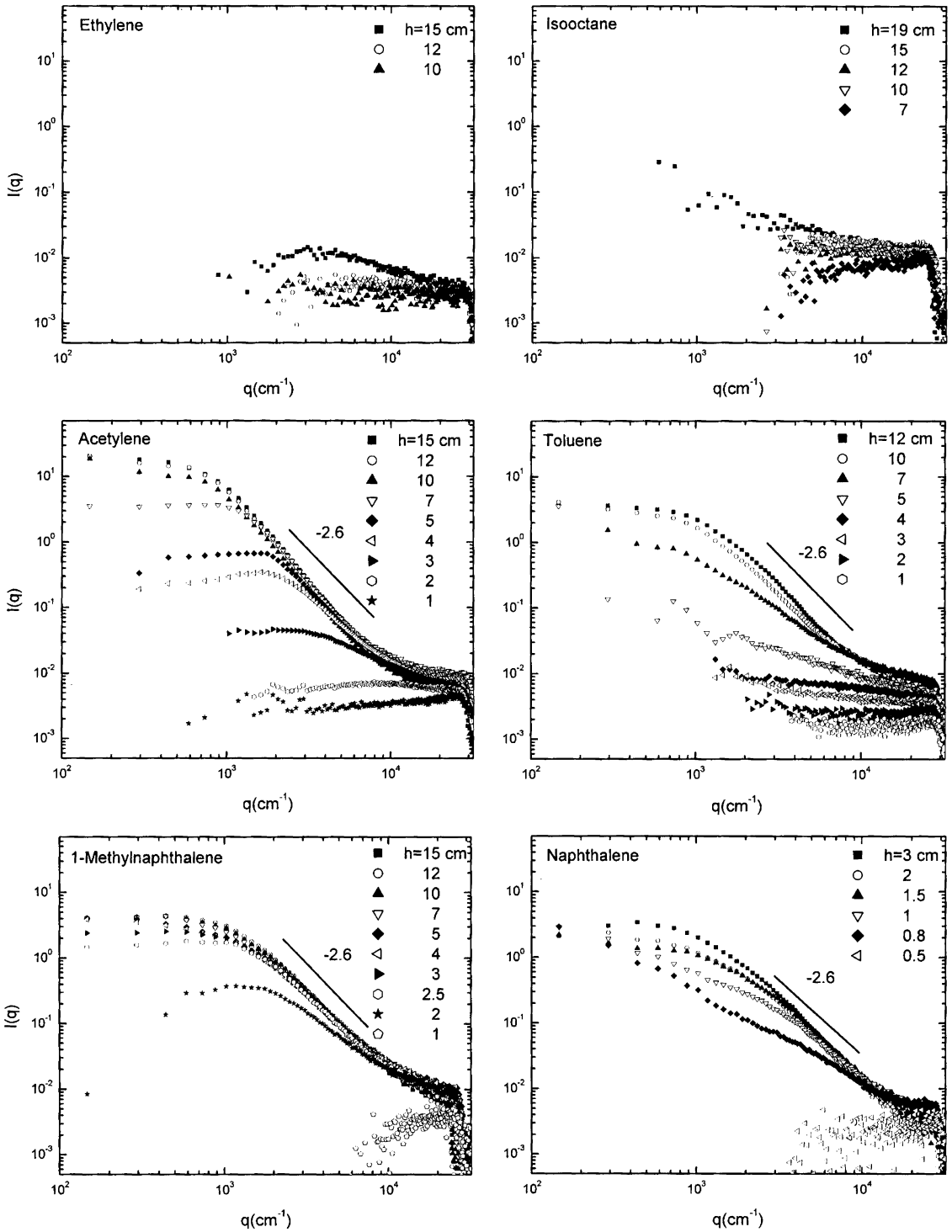

Figure 1. Scattered intensity versus scattering wave vector for six different fuels at different heights above the burner, *h*.

a fractal with dimension 2.55.[27] The light scattering data from the acetylene flame[14] showed both the $D \simeq 1.8$ morphology over submicron scales and the $D \simeq 2.6$ morphology in the supramicron range. Thus, we concluded that percolated superaggregates, *an aggregate of aggregates*, with fractal dimensions of 2.6 over the length scale from the DLCA aggregate size up to the overall superaggregate size formed in the flame. Now we find, as shown in Figure 1, that such superaggregates are not uncommon—they form in other flames as well.

We propose that the primary condition for the formation of percolated superaggregates of soot in a flame is a large soot volume fraction, f_v. To show this, we define the ideal gel point radius of gyration, $R_{g,G}$, as the size of the DLCA aggregates when they have grown large enough to percolate in three dimensions under the rough assumptions that they are spherical and the same size.[13,14,28] To a factor of order unity

$$R_{g,G} \simeq 1/2a f_v^{1/(D-3)} \quad (1)$$

where *a* is the primary particle radius. Equation 1 shows

(27) Stauffer, D.; Aharony, A. *Introduction to Percolation Theory*; Taylor and Francis: London, 1992.

(28) Fry, D.; Sintes, T.; Chakrabarti, A.; Sorensen, C. M. Enhanced Kinetics and Free Volume University in Dense Aggregating Systems. *Phys. Rev. Lett.* **2002**, *89*, 148301.

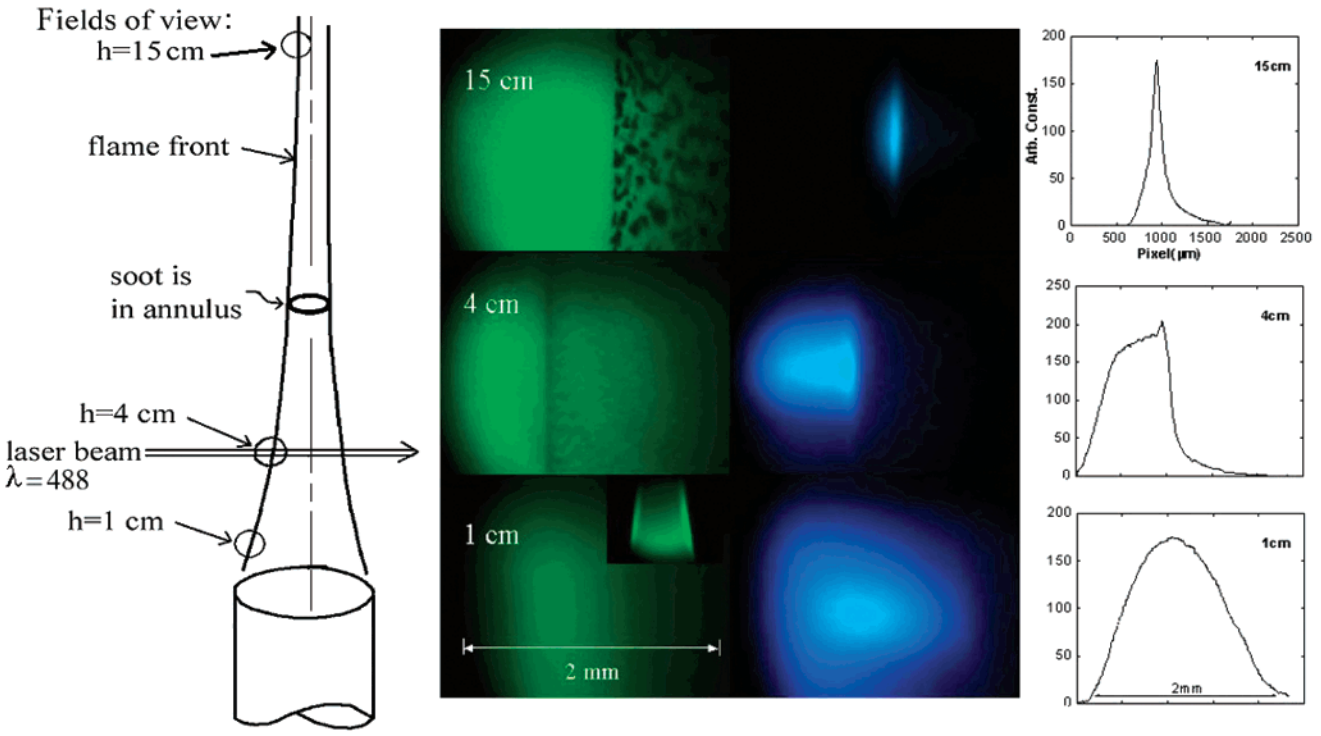

Figure 2. (left) Flame emanating from a cylindrical tube burner. The flame is an annular tube with vertical axis. The three fields of view at heights above the burner, h = 1, 4, and 15 cm, show schematically the positions of the images in the first column immediately to the right of the sketch. Note that the fields of view of these images show only the left side of the annular flame front. These images are for an acetylene/air diffusion flame and were taken by backlighting the flame with a 7 ns pulse from a Nd:YAG laser with $\lambda = 532$ nm. The inset in the 1 cm image shows the incandescence of the lower 2 cm of the flame. (middle) Pictures of the light scattered from an argon ion laser beam ca. 0.5 mm wide with λ = 488 nm directed through the flame and hence perpendicular to the soot region (the beam is parallel to the plane of the picture). This situation is shown schematically in the sketch on the far left for h = 4 cm. (right) Graphs of the scattered intensity of the middle panel.

that as f_v increases, $R_{g,G}$ decreases. A small $R_{g,G}$ means that the system will percolate rapidly. Before we calculate possible $R_{g,G}$ values, we describe two cooperative ways to achieve large soot volume fractions.

One way to achieve a large soot volume fraction, and hence the rapid formation of percolated superaggregates, is to burn a fuel with a large sooting tendency. Fuels have been ranked by their ability to form smoke, which is the emission of unburned soot from the top of the flame and directly related to the amount of soot formed. This ranking is[29]

naphthalenes > benzenes > alkynes > alkenes > alkanes (2)

Calcote and Manos[30] quantified smoking tendency with a threshold soot index (TSI). Table 1 gives the TSI values for the fuels we used as compiled by Olson et al.[31] Table 1 also specifies whether a given flame did or did not display superaggregates. Comparison of these data shows that the formation of superaggregates is correlated to sooting tendency specified either qualitatively through relation 2 or quantitatively through the TSI.

Observation of the flame geometry has led us to conclude that a large soot volume fraction can also be created if the flame front containing the soot narrows with increasing height above the burner. Figure 2 shows photographs of the edge of a acetylene/air diffusion flame and is typical of the other flames we studied. There we see both photographs of the flame backlit by a 7 ns pulsed Nd:YAG laser frequency doubled to $\lambda = 532$ nm (left column) and the scattering at $\theta = 90°$ of an argon ion laser at $\lambda = 488$ nm (middle column). Plots of this scattered intensity are also given (right column). These pictures show how the region of soot evolves from ca. 1.0 mm wide at a height of 1 cm above burner to very narrow at 15 cm. Although the reason for this compression of the soot layer is unknown to us, its consequence is to increase the soot volume fraction. For example, at a height above the burner of 1 cm, where the soot aggregates are small enough to allow a simple Rayleigh analysis of the extinction,[15] turbidity measurements indicate a volume fraction of soot of 8×10^{-5} for the acetylene flame. With this, $D = 1.8$, and a primary particle size of $a = 25$ nm,[32] eq 1 yields $R_{g,G} \simeq 30$ μm. Under the assumption that the soot volume remains constant upon increasing the height above the burner (it likely increases somewhat for these heavily sooting fuels), the compression of the soot region drives the soot volume fraction up. The amount of compression is difficult to determine because of the following: (1) The flame front appears to compress from the inside out and yield an anisotropic profile, as seen in Figure 2 for h = 4 cm. (2) We do not know how the length of a given segment of flame changes with increasing height, h. Given the more than order of magnitude compression between h =1 cm and h = 15 cm, we can estimate that f_v increases by a factor of 10, which would decrease $R_{g,G}$ to 4.5 μm, which is consistent with the onset of $D \simeq 2.6$ behavior in Figure 1. This rough argument succeeds in giving a viable,

(29) Glassmann, I. *Combustion;* Academic Press: New York, 1977.
(30) Calcote, H. F.; Manos, D. M. Effect of Molecular Structure on Incipient Soot Formation. *Combust. Flame* **1983**, *49*, 289−304.
(31) Olson, D. B.; Pickens, J. C.; Gill, R. J. The Effects of Molecular Structure on Soot Formation II. Diffusion Flames. *Combust. Flame* **1985**, *62*, 43−60.
(32) Sorensen, C. M.; Feke, G. D. The Morphology of Macroscopic Soot. *Aerosol Sci. Technol.* **1996**, *25*, 328−337.

semiquantitative agreement with observation that soot grows via three-dimensional DLCA, forming $D \simeq 1.8$ aggregates until they are large enough to percolate. If the soot volume fraction were smaller, as it is in flames such as ethylene and isooctane, and if the flame sheet did not compress, the large volume fractions of soot would not occur, and $R_{g,G}$ would be much larger, so much so that the DLCA soot could not evolve to the percolation point before it left the flame.

IV. Conclusion

This paper establishes that, regardless of origin, a previously unidentified phase of superaggregates forms in simple diffusion flames of fuels of high sooting tendency. The optical, radiative, transport, and absorptive properties of an aggregate are all strongly dependent on the fractal dimension. Hence, studies of these properties and their implications for soot detection and the effects of soot on our environment must contend with the presence of this new phase. Many other examples of heavily sooting and smoking flames are known. In many cases thin flame fronts occur at the boundaries between fuel-rich and oxygen-rich zones. Given the conditions of fuels with large sooting tendency and thin flame fronts, it is very likely that superaggregates of soot are being produced in those flames as well.

This work was supported by NSF Grant CTS 0080017 and NASA grant NAG3-2360.

LA036085+